

# Fast Hybrid Cascade for Voxel-based 3D Object Classification

Hui Cao

Jie Wang

Yuqi Liu

Siyu Zhang

Shen Cai✉

December 22, 2024

## Abstract

Voxel-based 3D object classification has been frequently studied in recent years. The previous methods often directly convert the classic 2D convolution into a 3D form applied to an object with binary voxel representation. In this paper, we investigate the reason why binary voxel representation is not very suitable for 3D convolution and how to simultaneously improve the performance both in accuracy and speed. We show that by giving each voxel a signed distance value, the accuracy will gain about 30% promotion compared with binary voxel representation using a two-layer fully connected network. We then propose a fast fully connected and convolution hybrid cascade network for voxel-based 3D object classification. This three-stage cascade network can divide 3D models into three categories: easy, moderate, and hard. Consequently, the mean inference time (0.3ms) can speedup about 5x and 2x compared with the state-of-the-art point cloud and voxel based methods respectively, while achieving the highest accuracy in the latter category of methods (92%). Experiments with ModelNet and MNIST verify the performance of the proposed hybrid cascade network.

## 1 Introduction

In the past several years, convolutional neural networks (CNNs) have been successfully applied to many computer vision directions, such as object recognition, detection and segmentation. Three-dimensional (3D) object recognition is an important task in 3D environment understanding, which can be used for a wide range of applications like self-driving vehicles and autonomous robots. Com-

pared to two-dimensional (2D) images, 3D data can provide rich geometrical information in three-dimensional space. Meanwhile, 3D data is usually acquired by depth cameras and lidar sensors, regardless of color, texture and illumination. Therefore, shape is the most important feature of three-dimensional objects, and its research is somewhat different from two-dimensional images. Traditional methods usually utilize 3D hand-crafted features, such as [24], and support vector machine (SVM) classifier to recognize the shape of an object. In recent years, many deep learning based approaches have been proposed to improve the classification performance of a certain 3D object representation.

The pioneering work MVCNN [28] attempts to apply 2D CNN on 3D shape analysis, which first renders a 3D object from several different view-points and extracts features from those 2D projections with 2D CNN feature extractor separately. Its variants include MVCNN-new [29] and RotationNet [10], etc. These image-based methods benefit from the existing well-developed network architectures, such as VGG [26] and ResNet [8], and achieve the best performance in 3D object classification. However, they are not geometrically intuitive and cannot easily be extended to other 3D tasks, such as part segmentation.

Another category of methods directly handle the surface point cloud of a 3D object. PointNet [22] consumes point clouds with a simple yet efficient MLP network. However, it only considers global features and ignores local neighborhood information, making it not suitable to fine-grained shape and complex scenes. Instead of working on individual points, PointNet++ [23] introduces a hierarchical neural network that applies PointNet recursively on the group points in different levels. To better utilize local geometric structure, DGCNN [32] constructs

a local neighborhood graph and applies edge convolutions on the connecting points to achieve a high accuracy.

Similar to point-based methods, volumetric CNNs can directly process 3D data. The difference is that volumetric methods first transfer an object to volumetric occupancy representation and then conduct 3D convolution on the voxel occupancy data. The early volumetric 3D CNNs are introduced in ShapeNet [33] and VoxNet [15], which achieve acceptable classification accuracy but are restricted by low resolution due to high memory and computation cost. To handle these problems, octree-based CNNs [31, 34, 11] propose to represent the object with a sparse grid-octree structure and implement 3D CNN on the octree grid voxel; [14] introduces binary weights in volumetric CNNs, which can reduce the calculation cost and accelerate the network by efficient bit-wise operations; [21] proposes several kinds of basis point sets (BPS) to efficiently reconstruct and classify 3D objects. The main problem of voxel-based methods is that the classification accuracy is obviously lower than that of surface point cloud ( $< 91\%$ ).

In this work, we propose a fast fully connected and convolution hybrid cascade network for voxel-based 3D object classification. The basic idea is that the proposed three-stage cascaded classifier can help identify three-dimensional objects quickly and with high accuracy. The example of 'sink' class in ModelNet40 test set is illustrated in Fig. 1 (a). The objects are divided into 'easy', 'moderate' and 'hard' sets through the three-stage cascaded classifier. It also can be seen in Fig. 1 (b) that the 'easy' set account for the majority of all samples, which can be credibly predicted by the first stage classifier. Since an 'easy' sample does not need to go through deeper stages, its computational cost is largely reduced.

The detailed hybrid cascade architecture is depicted in Fig. 2. The first stage classifier is a 2-layer fully connected network (FC-Net). The second and third classifiers are a shallow 3D CNN and a deep 3D CNN, respectively. When the top-1 classification score of a sample through the current classifier is lower than an adaptive threshold, the sample will be considered to be an uncertain shape and go through the latter classifier. Otherwise, this sample will be classified. 'C1', 'C2' and 'C3' actually corresponds to 'easy', 'moderate' and 'hard' categories, respectively. It is worth noting that the input signal we adopted is the signed distance field (SDF) of voxel,

rather than binary voxel. We experimentally find that the accuracy will gain about 30% promotion compared with binary voxel representation with the first FC-Net. For 3D CNN, the SDF voxel representation still gains an obvious promotion in accuracy. Therefore, thanks to the classification performance of SDF and the hybrid cascade architecture of three-stage classifier, the overall classification accuracy of the proposed method in ModelNet40 exceed all existing voxel-based methods and some point cloud based methods.

In summary, the contributions of our work can be concluded as follows:

- Based on the similarity analysis between character (MNIST) and 3D shape, we propose to directly use the SDF voxel for both FC-Net and 3D CNN, which promotes the classification performance of single network greatly.
- We propose a hybrid cascade architecture combining FC-Net with 3D CNN for voxel-based object classification, which improves the classification accuracy and decreases the mean inference time significantly.
- The proposed cascade strategy utilizes the adaptive threshold with confidence of each class to achieve high pass rate and high precision simultaneously.

## 2 Related Works

In this section, we will briefly review the previous works closely related to our work, including implicit representations of 3D shape, voxel-based 3D CNNs and cascade classifier.

### 2.1 Implicit Representations

In contrast to explicit representations which encode the shape discretely (e.g. voxels and surface points), implicit representations encode shapes continuously. Occupancy networks [7, 17] implicitly represent the 3D surface as the continuous decision boundary with a deep neural network classifier by inferring an occupancy probability. SDF is another popular choice for 3D shape representation. Voxel-based SDF representations have been extensively used for 3D shape completion [27, 20, 18]. In 3D

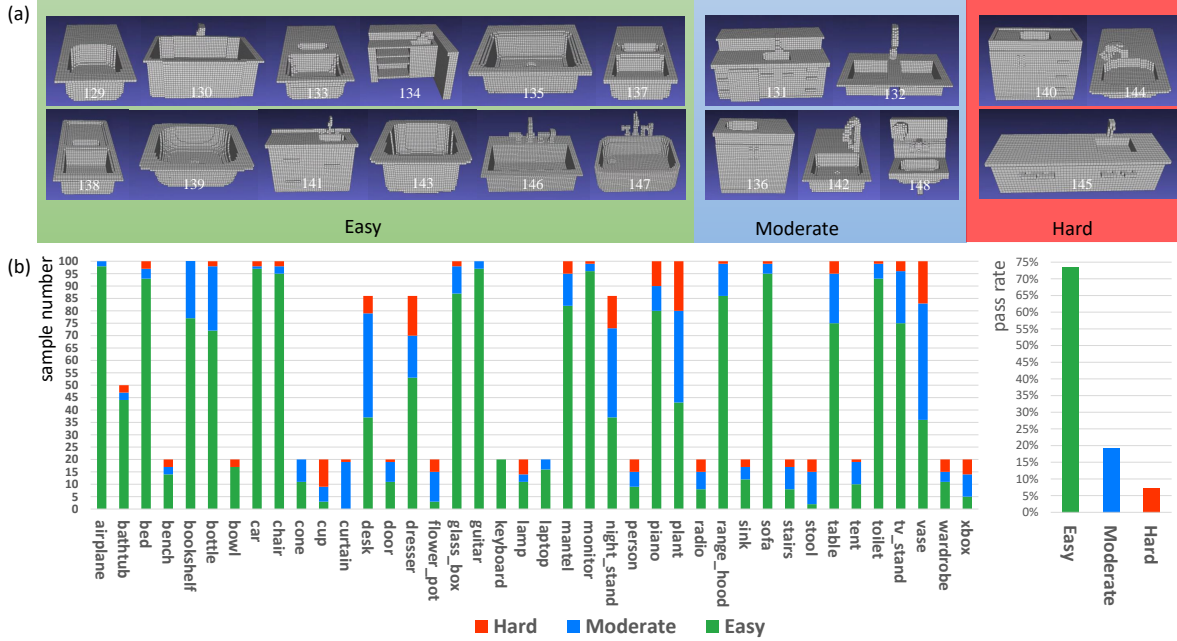


Figure 1: (a) Results of 'sink' class in ModelNet40 test set with model number through three-stage cascade network. 'Easy', 'Moderate', and 'Hard' categories are visually consistent with human classification. (b) two histograms of three categories. The left one plots sample numbers for each object class and difficulty category of ModelNet40. The right one depicts the pass rate of each difficulty category and reveals that more than 70% models can be inferred credibly in the first stage, which has large computing advantages.

object classification, [6] proposes to construct a class of more representative features named infilling spheres with SDF values as their radii and achieves better accuracy than PointNet [22] and PointNet++ [23].

## 2.2 Voxel based 3D CNNs

Early works of volumetric CNN [16, 33] propose to convert 3D shape to binary representation on voxel grids, and then apply a 3D convolution network to extract the global feature for shape analysis. However, they are unable to handle large scale scenes since the computation and memory cost grows with the cube of the resolution. To address the limits of high computation and memory cost, [14] transforms the inputs and parameters into binary values which largely accelerates the neural network by bit-wise operations. Another family of methods [31, 34, 11] represent the volumetric shape with octree structure, which require less computation and memory cost but achieve even

better accuracy in shape analysis tasks. [21] proposes to encode point clouds with a fixed-length feature vector of basis point sets (BPS), which can be computed efficiently with several standard neural network architectures. To our knowledge, the accuracy of BPS is the highest among all existing voxel-based methods.

## 2.3 Cascade Classifier

Cascade classifier has long been used in traditional object detection tasks, such as the classical Haar cascade classifier in face detection [30]. Cascade strategy is also introduced in object detection neural networks [19, 25], which train a sequence of detectors stage by stage with increasing IoU thresholds. Cascade detection networks often reject easy negative samples like background at early stages for better detection and faster inference. Since large number of obvious negative samples at early stages are discarded, it reduced the computational and memory cost

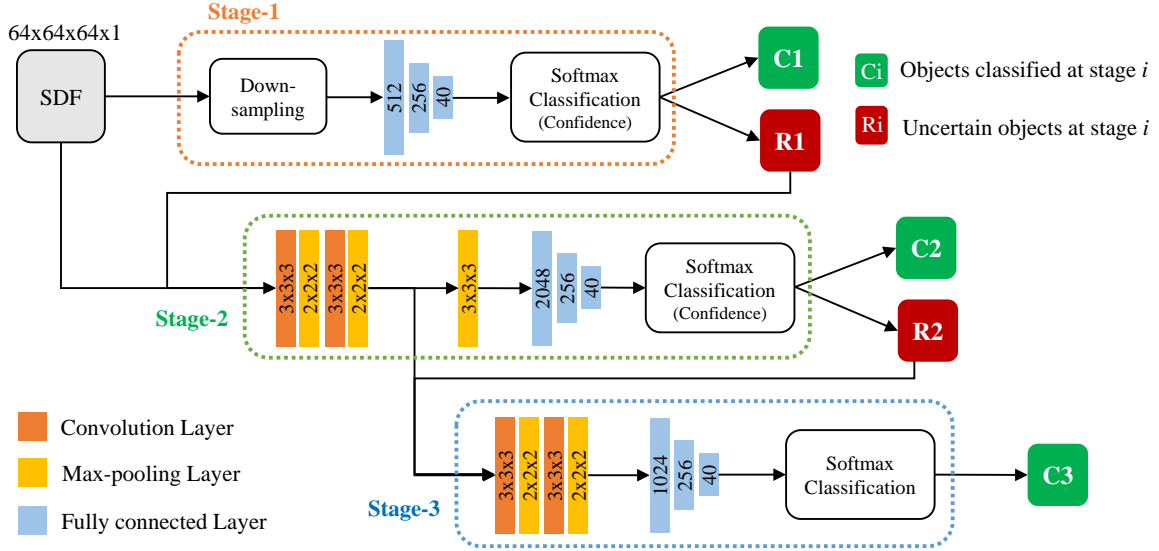


Figure 2: Hybrid cascade network architecture for SDF voxel classification.

because those discarded samples are not required to go through deeper layers. [9] uses a multi-scale network architecture and trains multiple classifiers with varying resource demands to improve the average accuracy. For semantic segmentation task, a deep layer cascade method is proposed [13] in which earlier convolution layers are trained to handle easy regions, and the harder regions are fed to the deep layers for segmentation.

### 3 Analysis from 2D MNIST Image to 3D Voxel

The MNIST dataset [1] contains 60000 training samples and 10000 test samples of handwritten digits from 0 to 9, which is often used for verifying machine learning techniques. The classification accuracy of MNIST with standard CNNs can achieve more than 99% by only taking gray pictures with the resolution of  $28 * 28$  as input [12]. Furthermore, even if using FC-Net on MNIST directly, the classification accuracy still seems to be acceptable (over 92% and 98% for 1 and 2 FC layers respectively). This phenomenon raises an important question. Can FC-Net be effective in the 3D object classification task?

Although FC-Net has been verified to be poor on other simple datasets such as CIFAR10 [2], we still presuppose that it may be effective for classifying 3D objects due to several common points between 2D MNIST images and 3D objects with voxel representation. First, both of them are arranged in order, which is beneficial to use FC-Net or CNN for classification. Moreover, both of them explicitly represent the geometric shape of an object including its silhouette (surface) and interior. The last commonality is both of the CNNs applied on them are very shallow (1-2 layers for MNIST and 2 layers for VoxelNet [15]). This also implies that even without convolution layers as feature extractor, 3D objects could be directly classified using FC-Net.

The experimental result of FC-Net on ModelNet [3] is shown in Table 1. The detailed setup is omitted here and will be demonstrated in Sec. 5. The overall classification accuracy of ModelNet10 and ModelNet40 with vanilla binary voxel representation (shown in the first row of Table 1) is smaller than 60% and 56%, respectively. But we experimentally found that the classification accuracy can be greatly improved by 30% if using the SDF value as voxel input (shown in the second row of Table 1). This is probably due to the fact that FC-Net is sensitive to the

proportion of the same input. When the input is converted to SDF, each voxel stores an distinguishable signed distance to implicitly represent the local shape, just like each pixel in gray image has a distinguishable gray value. Thus the performance can be greatly improved.

Another disadvantage of binary voxel representation is that its classification accuracy is obviously lower than that of surface point cloud. It is somewhat unreasonable because voxels already contain as much geometric information as point clouds. The third and fourth rows in Table 1 show that, when we use SDF value instead of binary input of voxel, classification accuracy is obviously improved, and exceeds the accuracy of the classic PointNet (89.2%) and PointNet++ (90.7%) with point coordinates as input.

To further illustrate the influence of different input forms, we also conduct several MNIST classification experiments with six different input signals including gray images, binary images, silhouette images, SDF images, and two simulated 3D MNIST models. One visual example is shown in Fig. 3. 3D MNIST models are simply produced through the stack of the same images in the third dimension, followed by zero-padding. This process is repeated 4 and 28 times for thin and thick 3D characters respectively. We test three different networks from shallow to deep to observe the performance of the above 2D inputs. As shown in Fig. 4, gray images achieve the highest accuracy in all networks except the 1-layer FC-Net. The accuracy of SDF images ranks second overall partly because of the visual similarity between SDF images and gray images. Moreover, as the neural network becomes shallower, the accuracy of the input with SDF signal has the minimal decrease. The experimental results of 3D MNIST are shown in Fig. 5. For thin 3D characters (4x), the classification accuracy of SDF voxel ranks only middle, slightly higher than the binary voxel. However, for thick 3D characters (28x), the accuracy of SDF voxel is significantly higher than other methods. This is because most of SDF values in 3D space of thin characters are almost the same, which constrains the performance of FC-Net.

It is worth noting that the validity of SDF representation has been proved in a recent work [21]. We independently verify the effectiveness of SDF representation in FC-Net and 3D CNN from another perspective before we have seen this work. Our concern mainly focuses on how to utilize the above characteristics of SDF representation

Table 1: Classification accuracy of FC-Net and CNN on ModelNet

Voxel Input	ModelNet10	ModelNet40
FC-Net		
Binary( $8^3$ )	59.91%	55.27%
SDF( $8^3$ )	92.40%	85.78%
3D CNN		
Binary( $64^3$ )	92.00%	87.20%
SDF( $64^3$ )	94.04%	90.76%

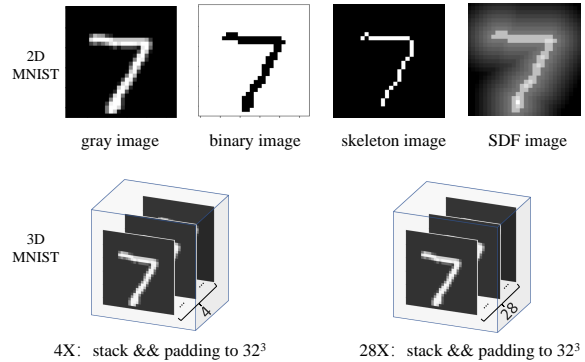


Figure 3: One example of different input signals of MNIST

to construct a fast cascade network for 3D voxel classification, which will be demonstrated in the next section.

## 4 The Hybrid Cascade Network for 3D Object Classification

Generally, most of the computational consumption in volumetric CNNs comes from the 3D convolution operations, while the parameters in FC layers dominate the memory and storage. Some volumetric methods are fast and avoid high memory and computation cost [16, 35], but are not able to achieve a relatively high recognition accuracy. Therefore, to find a balance between fast inference and high accuracy, we adopt the idea of cascade network and propose a fast fully connected and convolution hybrid

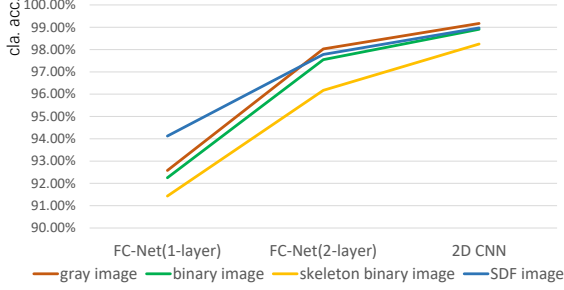


Figure 4: 2D MNIST comparison of different image inputs.

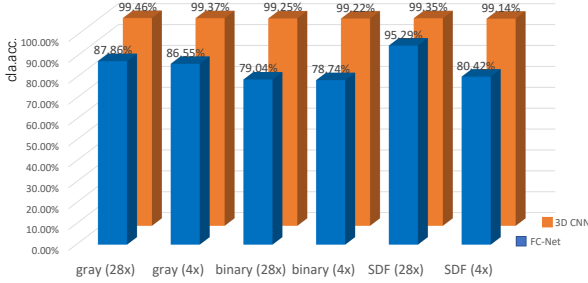


Figure 5: 3D MNIST comparison of different voxel inputs.

network for voxel-based 3D object classification.

An overview of our approach is illustrated in Fig. 2. Based on the analysis in Sec. 3, the FC-Net with SDF values as input at the first stage can classify simple objects very quickly. Then, 3D CNNs with 2 and 4 convolution layers are adopted at the second and third stages respectively to gain better performance.

## 4.1 Input Signal

Most volumetric CNN methods take binary signal as input and learn a probability distribution of binary variables on voxel grids, where 1 stands for object occupancy and 0 indicates the empty. Although the encouraging performance has been achieved, the accuracy of almost all methods are still lower than 90%. One basic factor leading to low classification accuracy is that binary volumetric representation could not provide detailed shape features for deep learning. In Sec. 3, we have performed several comparison experiments between different input signals and

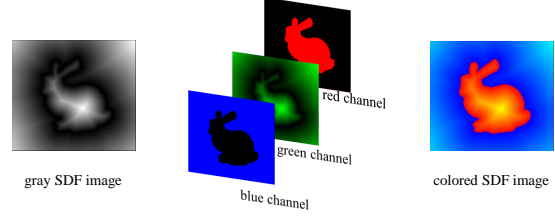


Figure 6: Example of colored SDF.

proved that SDF values behave much better than binary features in FC-Net and 3D CNN. Therefore, our further research mainly take SDF feature as input to improve the performance. The original voxel resolutions we use in this paper are  $16^3$ ,  $32^3$ ,  $64^3$ .

Besides the vanilla SDF input, we also propose to use colored SDF feature to further enrich the input, which is inspired by the pseudo-colorization method of gray images. Fig. 6 depicts one example of Bunny rabbit. From a human point of view, colored SDF images are more illustrative and may contain more prominent and easy-to-extract features. Experiments in Fig. 7 show its performance.

## 4.2 FC-Net

Although the nonlinear fitting ability of FC-Net with more than two hidden layers is very strong, it often fall into over-fitting. Therefore, FC-Net is now rarely used in various vision tasks. In this work, we construct a simple FC-Net with only two hidden layers to recognize the shape of a 3D voxel model. In order to reduce parameters and calculations, the voxel inputs are first down sampled to  $8 * 8 * 8$  at the equal intervals. Experiments in Sec. 5 show that considering SDF as input signal, the classification accuracy of FC-Net is satisfactory, whether it is used alone or in the first stage of the cascade classifier. Moreover, since the input data is down sampled to  $8*8*8$ , the network is not only very small, but also very fast. The pass rate problem of FC-Net in cascade classifier will be discussed in detail in Sec. 4.4.



### 4.3 3D CNN Stages

As illustrated in Fig. 2, if the output top-1 score of FC-Net at stage one is lower than an adaptive threshold, the voxel with the original resolution of the sample will be fed to the second classifier network which consists of two convolution blocks and a classification head similar to FC-Net. Specifically, the operation sequence “3D convolution + BN + ReLU + max-pooling” is adopted as a basic block. After the operation of two blocks, a max-pooling with size of 3 is performed to further down sample the feature volume from  $14*14*14*32$  to  $4*4*4*32$ , followed by feeding to the classification head of the second stage.

At the second stage, the comparison between the top-1 score and an adaptive threshold is performed again. If the score is lower than the threshold, the feature volume generated from the convolution block of the second stage will go through the third classifier. The third stage also contains two convolution blocks and a classification head similar to FC-Net. The main difference is the feature volume after two convolution blocks with the resolution of  $2*2*2*128$  is directly fed to the fully connected layers without max-pooling operation. The number of channels of the feature volume is doubly increased after each convolution block.

### 4.4 Hybrid Cascade Classifier Strategy

In this paper, the idea of cascade classifier network we adopt is similar to [13, 9]. Unlike the weak classifier adopted in other cascade works [30, 19, 25], the cascade classifier at each stage in our method is actually a strong classifier, which only classifies the objects with high confidence and leaves uncertain objects to next stage. When the softmax top-1 score of a sample is higher than the threshold  $\theta^t$  at stage  $t$  ( $t=1$  or  $2$ ), the prediction of the sample at this stage is considered to be reliable, otherwise the sample will go through the next classifier and perform the comparison again until the last stage.

Here the threshold  $\theta^t$  is not constant for each class, because the difficulty of classifying different classes of samples correctly is not same (see Fig. 1). Let  $\theta_C^t$  be the threshold of class  $C$  at the stage  $t$ . In order to maximize the inference speed and ensure the classification accuracy, the confidence  $p^t$  (common to each class) at stage  $t$  is introduced to adaptively determine the  $\theta_C^t$ . For each class

$C$ , the optimal  $\theta_C^{t*}$  in theory is expressed by

$$\theta_C^{t*} = \arg \max_{\theta_C^t} (N_C^+(\theta_C^t)), \quad (1)$$

$$s.t. \quad \frac{N_C^+(\theta_C^t)}{N_C^+(\theta_C^t) + N_C^-(\theta_C^t)} \geq p^t \quad (2)$$

where  $N_C^+$  and  $N_C^-$  denote the number of positive and negative samples of one class whose top-1 scores are bigger than  $\theta_C^t$ , respectively. Given a specified confidence  $p^t$ ,  $N_C^+$  and  $N_C^-$  should satisfy the above confidence constraint. However, in practice, we find that according to the threshold configuration of the above equations, the highest accuracy cannot always be achieved. This is because the negative sample distribution of each class for different classifiers is not the same. Therefore, simply throwing the negative samples of each class according to a common confidence standard to the subsequent classifier will decrease the accuracy. A revised standard is given by

$$\theta_C^{t*} = \arg \max_{\theta_C^t} (N_C^+(\theta_C^t)), \quad (3)$$

$$s.t. \quad \frac{N_C^+(\theta_C^t) - N_C^+(\theta_C^t)|_{p^t=1.0}}{N_C^+(\theta_C^t) - N_C^+(\theta_C^t)|_{p^t=1.0} + N_C^-(\theta_C^t)} \geq q^t \quad (4)$$

where  $N_C^+(\theta_C^t)|_{p^t=1.0}$  denotes the maximum number that all pass samples of each class are correct with a specific threshold  $\theta_C^t|_{p^t=1.0}$ . The number  $N_C^+(\theta_C^t) - N_C^+(\theta_C^t)|_{p^t=1.0}$  represents the incremental changes of positive samples, as the threshold decreases.  $N_C^-(\theta_C^t)$  represents the number of incremental changes of negative samples.  $q^t$  denotes the incremental confidence which is more effective for improving accuracy. As a result, more samples will be classified at early stage, which can further improve the classification accuracy and speed up the inference time.

Let  $\eta_C^t$  be the top-1 score of a sample classified by class  $C$  at the stage  $t$ . If the value  $\eta_C^t$  is greater than  $\theta_C^t$ , this sample will be predicted credibly by the classifier at stage  $t$ . Otherwise, this sample will be fed to the next classifier. Let  $\lambda^1$  and  $\lambda^2$  be the pass rates of ‘easy’ and ‘moderate’ samples classified by stage 1 and stage 2 respectively to the whole test set. The mean inference time is given by:

$$T_{mean} = 1 * T^1 + (1 - \lambda^1) * T^2 + (1 - \lambda^1 - \lambda^2) * T^3 \quad (5)$$

where  $T_i, i = 1, 2, 3$  denotes the inference time of stage  $i$  in Fig. 2. It is clear that, to achieve the fast inference, the ratios  $\lambda^1$  and  $\lambda^2$  should be increased as much as possible under the confidence constraint.

## 4.5 Training Model of Cascade Network

In the training process, classifiers at three stage are trained separately in order. In particular, FC-Net is completely independently trained without sharing any layers with the other two stages. While stage three shares part of convolution layers with the second stage. Once the training of the early classifiers has finished, the network parameters are frozen until the latter classifiers finish training. Therefore, as the two networks share part of network parameters, if the previous network has completed training, the latter network no longer needs to train the parameters in the shared layers.

The values of the two confidence thresholds at each stage are given as hyper-parameters in our experiments and the optimal thresholds were automatically determined by testing multiple threshold combinations on the test set. The classification results of several combination of the two thresholds are shown in Table 2. This method of choosing the optimal threshold combinations is similar in principle to testing network parameters of different epochs on the test set, which can further improve the classification accuracy of the cascade network.

## 5 Experiments

Our experimental conditions are listed as follows:

*Dataset:* ModelNet10, ModelNet40, MNIST, and 3D MNIST(self-generated).

*Software Environment:* PyTorch 1.2.0 + CUDA 10.

*Hardware:* Intel 9900K CPU + 16G Memory + NVIDIA 2080TI GPU.

To verify the effectiveness of the proposed SDF voxel and the performance of the hybrid cascade network, we design several kinds of experiments, including MNIST

classification, individual classification of three stages, hybrid cascade classification, and ablation classification. **All source codes have been packaged in the supplementary material and will be released online.**

### 5.1 Data Pre-processing

**Gray SDF.** The ModelNet40 dataset contains 12,311 CAD models from 40 classes and is split to 9843 training set and 2468 test set. Specifically, the ModelNet10 dataset contains 4899 CAD models from 10 categories, which are parts of the ModelNet40 dataset. To obtain the SDF form of ModelNet40 and ModelNet10, first, we need to normalize each CAD model to a unit ball and transform it to a volumetric model through the solid voxelization method in PyMesh library [4]. Then, we calculate the SDF of each voxel whether it is inside or outside the object by utilizing another C++/python library named edt [5]. The positive SDF means the distance from the exterior voxel grid to its closest surface while the negative SDF means the distance from the interior voxel grid to its closest surface. Before training, the positive and negative SDF values have been normalized to  $[0, 1]$  and  $[-1, 0]$  respectively.

**Colored SDF.** Colored SDF is consisted of three gray images as R, G and B channels. One example is illustrated in Fig. 6. Red and blue channels denote the interior and the exterior of an object respectively, and both of them are drawn with a single color. A revised gray SDF is applied in the green channel, where the gray value at the edge is set to 0 to enhance visual appeal.

**3D MNIST.** 3D MNIST models are simply produced by stacking a number of 2D MNIST gray and SDF images in space, and then being padded to  $32^3$  with zero for fair use of 3D CNN. In our work, the number of stacked images is 4 and 28 for thin and thick 3D characters respectively, as illustrated in Fig. 3.

### 5.2 MNIST Classification

In MNIST classification experiments, besides the original MNIST images with resolution  $28 * 28$ , other variants including binary images, silhouette images, and SDF images are also used as inputs of FC-Net and 2D CNN. One example has been shown in Fig. 3. For 2D MNIST classification, we test the performance of 1-layer FC-Net(784,10), 2-layer FC-Net(784,128,10) and a 2D CNN



which contains two convolution layers and two fully-connected layers. The experimental results have been shown in Fig. 4. Gray images achieve the highest accuracy in all networks except in the 1-layer FC-Net. The accuracy of SDF values as input ranks second overall partly because of the visual similarity between SDF images and gray images. Moreover, as the neural network becomes shallower, the accuracy of the input with SDF signal has the minimal decrease.

Note that the accuracy of 3D MNIST shown in Fig. 5 is a little better than 2D MNIST, which implies that 3D convolution is as effective as 2D convolution, at least for this scenario.

### 5.3 Individual Classification of Three Stages

Before demonstrating the performance of the hybrid cascade method, we first test the performance of the individual network at each stage. At the same time, multiple SDF inputs are sent into the network to compare the performance differences. The results are depicted in Fig. 7. The single network at the third stage achieves the highest recognition accuracy among these three networks, but costs the longest inference time. The performance of colored SDF voxel is worse than gray SDF voxel at the early two stages but better than that at stage 3. For a single stage network, it is difficult to balance fast inference speed and high precision at the same time. Meanwhile, the accuracy is still not optimal considering that the cascade classifiers could complement each other.

### 5.4 Cascade Classification

In the proposed hybrid cascade network, the important parameters that affect final performance are confidences  $p^1$ ,  $p^2$ ,  $q^1$ ,  $q^2$ . Table 2 shows the numbers of pass and correct samples at stage 1 and 2 on ModelNet40 with different combinations of confidences. From Table 2, it is clear that a trade-off have to be made between pass rates, inference speed and accuracy of each stage. We finally choose  $q^1 = 0.8$ ,  $q^2 = 0.66$  in our cascade network for ModelNet40. The results are shown in Table 3. It can be seen that the overall accuracy of the proposed method with gray SDF voxel as input surpasses BPS-Conv3D [21]

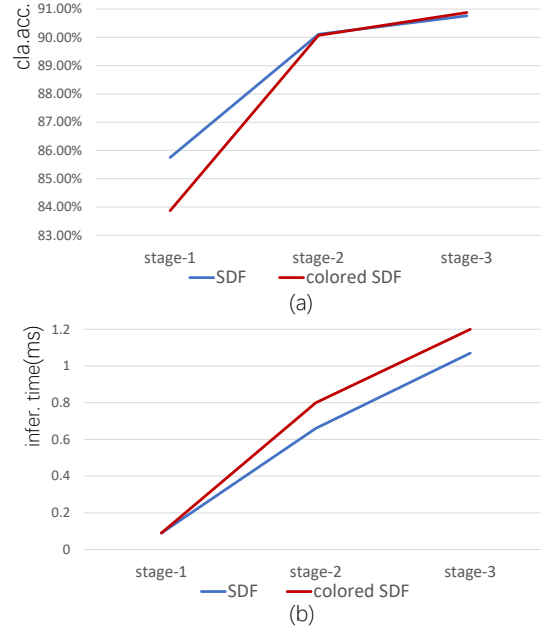


Figure 7: Accuracy and speed of the individual network at three stages with two kinds of SDF inputs. (a) accuracy results. (b) speed results.

which uses BPS grids with direction information as input while maintaining about half of the inference time.

### 5.5 Ablation

After demonstrating the performances of individual network at three stages, the cascade network, multiple SDF inputs and multiple combination of confidences of stage 1 and 2, ablation experiments focus on the performance when stage 1 or stage 2 is removed from the hybrid cascade architecture. Table 4 shows that with the removal of the first stage, the accuracy drops a little but the average inference time rises to 0.72ms. The reason is that stage 1 classifies 73.5% test samples and the inference time only costs 0.09ms, which is much smaller than that of stage 2 and 3. Besides, with the removal of the second stage, the accuracy suffers a larger loss compared with the removal of the first stage, but the increase of inference time is subtle.

Table 2: Study on different combinations of confidences.

Confidence	$p^1 = 1$ $p^2 = 1$	$p^1 = 0.98$ $p^2 = 0.98$	$p^1 = 0.96$ $p^2 = 0.96$	$q^1 = 0.9$ $q^2 = 0.9$	$q^1 = 0.8$ $q^2 = 0.8$	$q^1 = 0.8$ $q^2 = 0.66$
stage-1	1281/1281	1378/1368	1612/1572	1560/1549	1815/1770	1815/1770
stage-2	440/440	403/401	327/324	408/402	316/300	473/414
Accuracy	91.77%	91.65%	91.36%	91.97%	91.73%	92.01%

Table 3: Accuracy, parameters, flops and forward time of different methods.

Method	Input signal	Accuracy (%)	Params	Flops	Infer. time
MVCNN-new(12x) [28]	images	<b>95.0</b>	$1.3 \times 10^8$	$9.0 \times 10^{10}$	13.5 ms
PointNet [22]	xyz	89.2	$3.5 \times 10^6$	$4.4 \times 10^8$	1.8 ms
PointNet++ [23]	xyz	90.7	$1.7 \times 10^6$	$1.6 \times 10^9$	2.9 ms
DGCNN [32]	xyz	92.2	$1.8 \times 10^6$	$2.5 \times 10^9$	3.5ms
Voxnet [16]	binary voxel	83.0	$9.0 \times 10^5$	$6.0 \times 10^7$	<b>0.25 ms</b>
BPS-Conv3D[21]	BPS grids+dire.	90.8	$4.4 \times 10^6$	$3.5 \times 10^8$	0.55ms
Ours (cascade classifier)	SDF voxel	92.0	$1.2 \times 10^6$	$5.7 \times 10^8$	0.30ms

Table 4: Ablation results of removing one stage.

Ablation Operation	Accuracy	Avg. infer. time
Remove stage-1	91.7%	0.72ms
Remove stage-2	91.5%	0.37ms

## 6 Conclusion

In this paper, we present a three-stage cascade network for 3D object classification. The accuracy of the proposed network exceeds all existing voxel-based methods and is close to the state-of-the-art point cloud based methods. Meanwhile, the inference speed of this cascade network is also the fastest among all high-performance methods. There are several reasons for the excellent performance of the proposed cascade network. First, the network input we adopt is the SDF voxel instead of the traditional binary voxel. Second, the hybrid cascade classifier integrates the advantages of FC-Net and 3D CNNs to achieve better performance than an individual network. Third, the use of an adaptive threshold under the incremental confidence fur-

ther improves the classification accuracy. Although the overall accuracy of the deeper network is better than that of the shallower network, for part of harder samples, the recognition rate of the shallower network is higher than that of the deeper network.

## References

- [1] <http://yann.lecun.com/exdb/mnist/>. 4
- [2] <http://www.cs.toronto.edu/~kriz/cifar.html>. 4
- [3] <https://modelnet.cs.princeton.edu/>. 4
- [4] <https://github.com/PyMesh/PyMesh/>. 8
- [5] <https://pypi.org/project/edt/>. 8
- [6] H. Cao, H. Du, S. Zhang, and S. Cai. Inspherenet: a concise representation and classification method for 3d object. *International Conference on Multimedia Modeling (MMM)*, pages 327–339, 2020. 3
- [7] Z. Chen and H. Zhang. Learning implicit fields for generative shape modeling. *IEEE Conference on Computer Vision and Pattern Recognition (CVPR)*, pages 5932–5941, 2019. 2
- [8] K. He, X. Zhang, S. Ren, and J. Sun. Deep residual learning for image recognition. *IEEE Conference on Computer*

- Vision and Pattern Recognition (CVPR)*, pages 770–778, 2016. [1](#)
- [9] G. Huang, D. Chen, T. Li, F. Wu, L. van der Maaten, and K. Q. Weinberger. Multi-scale dense networks for resource efficient image classification. *International Conference on Learning Representations (ICLR)*, 2018. [4](#), [7](#)
- [10] A. Kanazaki, Y. Matsushita, and Y. Nishida. Rotationnet: Joint object categorization and pose estimation using multiviews from unsupervised viewpoints. *IEEE Conference on Computer Vision and Pattern Recognition (CVPR)*, pages 5010–5019, 2018. [1](#)
- [11] R. Klokov and V. S. Lempitsky. Escape from cells: Deep kd-networks for the recognition of 3d point cloud models. *IEEE International Conference on Computer Vision (ICCV)*, pages 863–872, 2017. [2](#), [3](#)
- [12] Y. Lecun, L. Bottou, Y. Bengio, and P. Haffner. Gradient-based learning applied to document recognition. *Proceedings of the IEEE*, 86(11):2278–2324, 1998. [4](#)
- [13] X. Li, Z. Liu, P. Luo, C. C. Loy, and X. Tang. Not all pixels are equal: Difficulty-aware semantic segmentation via deep layer cascade. *IEEE Conference on Computer Vision and Pattern Recognition (CVPR)*, pages 6459–6468, 2017. [4](#), [7](#)
- [14] C. Ma, Y. Guo, Y. Lei, and W. An. Binary volumetric convolutional neural networks for 3-d object recognition. *IEEE Transactions on Instrumentation and Measurement*, 68(1):38–48, 2019. [2](#), [3](#)
- [15] D. Maturana and S. Scherer. Voxnet: A 3d convolutional neural network for real-time object recognition. *IEEE/RSJ International Conference on Intelligent Robots and Systems*, pages 922–928, 2015. [2](#), [4](#)
- [16] D. Maturana and S. A. Scherer. Voxnet: A 3d convolutional neural network for real-time object recognition. *2015 IEEE/RSJ International Conference on Intelligent Robots and Systems (IROS)*, pages 922–928, 2015. [3](#), [5](#), [10](#)
- [17] L. M. Mescheder, M. Oechsle, M. Niemeyer, S. Nowozin, and A. Geiger. Occupancy networks: Learning 3d reconstruction in function space. *IEEE Conference on Computer Vision and Pattern Recognition (CVPR)*, pages 4455–4465, 2019. [2](#)
- [18] M. Michalkiewicz, J. K. Pontes, D. L. Jack, M. Baktash, and A. Eriksson. Implicit surface representations as layers in neural networks. *IEEE International Conference on Computer Vision (ICCV)*, pages 4742–4751, 2019. [2](#)
- [19] W. Ouyang, K. Wang, X. Zhu, and X. Wang. Chained cascade network for object detection. *IEEE International Conference on Computer Vision (ICCV)*, pages 1956–1964, 2017. [3](#), [7](#)
- [20] J. J. Park, P. Florence, J. Straub, R. A. Newcombe, and S. Lovegrove. Deepsdf: Learning continuous signed distance functions for shape representation. *IEEE Conference on Computer Vision and Pattern Recognition (CVPR)*, pages 165–174, 2019. [2](#)
- [21] S. Prokudin, C. Lassner, and J. Romero. Efficient learning on point clouds with basis point sets. *IEEE International Conference on Computer Vision (ICCV)*, pages 4331–4340, 2019. [2](#), [3](#), [5](#), [9](#), [10](#)
- [22] C. R. Qi, H. Su, K. Mo, and L. J. Guibas. Pointnet: Deep learning on point sets for 3d classification and segmentation. *IEEE Conference on Computer Vision and Pattern Recognition (CVPR)*, pages 77–85, 2017. [1](#), [3](#), [10](#)
- [23] C. R. Qi, L. Yi, H. Su, and L. J. Guibas. Pointnet++: Deep hierarchical feature learning on point sets in a metric space. In *Advances in neural information processing systems (NIPS)*, 2017. [1](#), [3](#), [10](#)
- [24] R. B. Rusu, N. Blodow, and M. Beetz. Fast point feature histograms (fpfh) for 3d registration. *IEEE International Conference on Robotics and Automation*, pages 3212–3217, 2009. [1](#)
- [25] S. Shivajirao, R. Hantach, S. B. Abbès, and P. Calvez. Mask r-cnn end-to-end text detection and recognition. *IEEE International Conference On Machine Learning And Applications (ICMLA)*, pages 1787–1793, 2019. [3](#), [7](#)
- [26] K. Simonyan and A. Zisserman. Very deep convolutional networks for large-scale image recognition. In *International Conference on Learning Representations (ICLR)*, May 2015. [1](#)
- [27] D. Stutz and A. Geiger. Learning 3d shape completion from laser scan data with weak supervision. *IEEE Conference on Computer Vision and Pattern Recognition (CVPR)*, pages 1955–1964, 2018. [2](#)
- [28] H. Su, S. Maji, E. Kalogerakis, and E. G. Learned-Miller. Multi-view convolutional neural networks for 3d shape recognition. *IEEE International Conference on Computer Vision (ICCV)*, pages 945–953, 2015. [1](#), [10](#)
- [29] J.-C. Su, M. Gadelha, R. Wang, and S. Maji. A deeper look at 3d shape classifiers. *ArXiv*, abs/1809.02560, 2018. [1](#)
- [30] P. A. Viola and M. J. Jones. Rapid object detection using a boosted cascade of simple features. *Computer Society Conference on Computer Vision and Pattern Recognition (CVPR)*, 1:I–I, 2001. [3](#), [7](#)
- [31] P. Wang, Y. Liu, Y. Guo, C. Sun, and X. Tong. O-cnn: octree-based convolutional neural networks for 3d shape analysis. *ACM Transactions on Graphics*, 36(4):72, 2017. [2](#), [3](#)
- [32] Y. Wang, Y. Sun, Z. Liu, S. E. Sarma, M. M. Bronstein, and J. M. Solomon. Dynamic graph cnn for learning on point

- clouds. *ACM Transactions on Graphics*, 38:146:1–146:12, 2019. [1](#), [10](#)
- [33] Z. Wu, S. Song, A. Khosla, F. Yu, L. Zhang, X. Tang, and J. Xiao. 3d shapenets: A deep representation for volumetric shapes. *IEEE Conference on Computer Vision and Pattern Recognition (CVPR)*, pages 1912–1920, 2015. [2](#), [3](#)
- [34] Y. Yuan and J. Wang. Ocnet: Object context network for scene parsing. *ArXiv*, abs/1809.00916, 2018. [2](#), [3](#)
- [35] S. Zhi, Y. Liu, X. Li, and Y. Guo. Toward real-time 3d object recognition: A lightweight volumetric cnn framework using multitask learning. *Computers & Graphics*, 71:199–207, 2017. [5](#)